Italian Journal of Agrometeorology
Rivista Italiana di Agrometeorologia

Firenze University Press
www.fupress.com/ijam

OPEN ACCESS

Citation: A. Farashi, Z. Karimian (2021) Predicting the potential habitat of Russian-Olive (*Elaeagnus angustifolia*) in urban landscapes. *Italian Journal of Agrometeorology* (1): 3-19. doi: 10.36253/ijam-1071

Received: September 5, 2020

Accepted: November 14, 2020

Published: August 9, 2021

Data Availability Statement: All relevant data are within the paper and its Supporting Information files.

Competing Interests: The Author(s) declare(s) no conflict of interest.

Funding: This study was funded by the Vice-Presidency for Science and Technology of Iran (grant number 96002787).

Author contributions statement: All authors contributed to the study conception and design. Material preparation, data collection and analysis were performed by Azita Farashi and Zahra Karimian. The first draft of the manuscript was written by Azita Farashi and all authors commented on previous versions of the manuscript. All authors read and approved the final manuscript.

Predicting the potential habitat of Russian-Olive (*Elaeagnus angustifolia*) in urban landscapes

Azita Farashi[1], Zahra Karimian[2]

[1] *Department of Environmental Sciences, Faculty of Natural Resource and Environment, Ferdowsi University of Mashhad, Mashhad, Iran*
[2] *Department of Ornamental Plants, Research Center for Plant Sciences, Ferdowsi University of Mashhad, Iran*
E-mail: farashi@um.ac.ir; zkarimianf@gmail.com

Abstract. Russian-olive *(Elaeagnus angustifolia)* is a species native to southern Europe and central and eastern Asia. This species plays an important role in urban landscape design because of its rapid growth, resistance in harsh climates and tolerance to human-caused pressure. Understanding its potential dispersal and restricting parameters are the first steps toward the sustainable use of this species. Here, we used Species Distribution Models to predict the potential distribution of Russian-olive in Iran climate and estimate the possible limiting factors for its spread. Our results highlighted the importance of environmental variables including climatic factors, soil, and lithology in the distribution of this species throughout the country. According to these results, suitable habitats for Russian-olive are located in the north of Iran along the Alborz and Koppeh-Dagh mountain ranges. Therefore, the suitable habitats for this species are limited to only nine percent of the country. A habitat suitability map can be used to evaluate future developments in urban areas and predict the dispersal range of Russian-olive in Iran. Our results show that Russian-olive can be used to create new green spaces in urban climates in the northern regions of Iran.

Keywords: climate, green space, ornamental tree, SDM, urban areas.

INTRODUCTION

The Middle East and North Africa are home to five percent of Earth's human population. However, only one percent of the global freshwater resources is located in Middle Eastern and North African countries (Djuma et al. 2016). As a result, water scarcity looms large across the region (Al-Ansari and Knutsson 2011; Al-Ansari et al. 2014; Abbas et al. 2018). To complicate the problem even further, population growth and political tensions threaten the sustainability of existing water resources in the Middle East and North Africa (Djuma et al. 2016).

Consequently, making use of different water sources and enhancing the resilience of water supply is crucial to meet the needs of the increasing urban population (Bichai et al. 2015). The environmental damage associated with urban development has drawn attention to the need for green spaces in cities, which will lead to increased water use (Zhang et al. 2017). Green spaces are among the indicators of sustainable urban development. When planning for urban green spaces, numerous elements, such as economic, political, social, and cultural factors, along with management and planning considerations need to be taken into account (Haq 2011). Conservation of biological resources and maintaining soil and water quality are among the services provided by urban green spaces (Haq 2011, 2015). Many studies indicate that plant particularly trees can improve the urban microclimate and influence thermal comfort in various ways including shading, controlling the humidity, wind break, pollutant absorption and produce oxygen (Abreu- Harbich et al. 2015; Thoma et al. 2016; Afshar et al., 2018).

In arid regions such as the Middle East, design of urban green spaces is one of the main challenges facing city planners and urban architects. One solution to address this challenge is the use of native plant species which are adapted to the dry conditions of the region (Katz and Shafroth 2003; Kiseleva and Chindyaeva 2011).

The first step in utilizing native species is identification of their habitat requirements. Species distribution models (SDMs) trace their origin to the 1970s and have remained a common tool for ecologists throughout the following decades (e.g., Guisan and Zimmermann 2000; Guisan and Thuiller 2005; Rooper et al. 2016). In the time since their conception, several SDM algorithms have been developed, as discussed by Elith and Leathwick (2009) and Farashi and Alizadeh-Noughani (2018). These algorithms distinguish the major variables that determine a species' suitable habitat and show how predictor variables impact response variables. Furthermore, SDM algorithms enable researchers to see species' potential distribution (Liang and Stohlgren, 2011; Liang et al. 2017). Through modifications, these algorithms have been optimized for use in fields such as biogeography, ecology, evolution, and species conservation and management (Mikolajczak et al., 2015; Hannah et al., 2015). SDMs have also been used to assess the potential distribution of plant species (e.g., Kumar and Stohlgren 2009; Hemsing and Bryn 2012; Zhang et al., 2013; Guida et al. 2014; Hu et al. 2018). In the present study, we have used SDMs to predict the spatial distribution of Russian-olive (*Elaeagnus angustifolia*), a native plant species in Iran. Iran is a Middle Eastern country located on Earth's arid belt with upwards 60% of the country's area having an arid or semi-arid climate. In areas that receive little precipitation and experience severe fluctuations from year to year, agriculture is often limited by water availability (Modarres and da Silva 2007).

Russian-olive is native to Eurasia that occurs on coasts, in riparian areas, along watercourses, in other relatively moist habitats and also in many arid and semiarid regions of the world (Klich, 2000; Peterson et al., 2003). Soil salinity (low to medium concentrations), pH and water supply and moisture (low) are important environmental factors in Russian-olive habitat (Carman, 1982; Zitzer and Dawson, 1992; Reynolds and Cooper, 2010; Dubovyk et al., 2016). Russian-olive is resistant to drought (+46 °C) and frost (-46 °C) (Stratu et al., 2016; Akbolat et al., 2008). This tree is an ecologically valuable plant that are adapted to a variety of harsh conditions such as cold, drought, and salinity or alkalinity of soil (Asadiar et al. 2013; Zhang et al. 2018). The species endures through water scarcity by using groundwater (Katz and Shafroth 2003). Along with its desirable ecological characteristics, Russian-olive possess aesthetic values such as its beautiful oval crown, arching branches, silver leaves and shiny dark red fruits. Therefore *E. angustifolia* is particularly suitable for urban landscapes in arid regions such as Iran. This tree can be used to create sustainable green spaces in urban climates of Iran.

MATERIALS AND METHODS

Study area and species

Iran is located in Western Asia between 24°-40° N and 44°-64° E. Due to its habitat diversity and phytogeographic variety, Iran hosts rich biodiversity. Over 8,000 species of plants are found in Iran, of which 1,810 are endemic (Ghahraman and Attar 2000; Willis 2001). Russian-olive is a deciduous tree, sometimes with a shrubby habit, in the family Elaeagnaceae (Saboonchian et al. 2014). This species naturally grows in central and eastern Asia and southern Europe. Russian-olive grows quickly, reaching a maximum height of 10 m and maximum trunk diameter of 30 cm. Trees usually bear fruit after 5-6 years (Katz and Shafroth 2003).

Species distribution models

SDMs were developed in Biomod2 package (Thuiller et al. 2009, 2014) in R version 3.1.25 (R Core Team 2014). 10 different algorithms were used to study the species (Tab. 1). The algorithms can be categorized as: regression, machine learning, classification and enveloping algorithms. Regression-based algorithms include generalized linear models (GLMs) and generalized additive models (GAMs) which generate linear and non-linear equations between presence data and environmental variables, respectively. Machine learning algorithms include artificial neural networks (ANN), boosted regression trees, (BRT), multivariate adaptive regression splines (MARS), maximum

Table 1. The SDM algorithms in biomod² used in this study.

SDM	Variable	Type	Reference	TSS
ANN	Artificial neural networks	P/A	Lek and Guégan (1999)	0.71
BRT	Boosted regression trees	P/A	Elith et al. (2008)	0.71
CART	Classification and regression trees	P/A	Vayssières et al. (2000)	0.60
FDA	Flexible discriminant analysis	P/A	Hastie et al. (1994)	0.72
GAM	Generalized additive models	P/A	Guisan et al. (2002)	0.60
GLM	Generalized linear models	P/A	Guisan et al. (2002)	0.70
MaxEnt	Maximum entropy	P/B	Phillips et al. (2006)	0.80
MARS	Multivariate adaptive regression splines	P/A	Friedman (1991)	0.61
RF	Random forest	P/A	Breiman (2001)	0.65
SRE	Surface range envelope	P/B	Busby (1991)	0.65
Ensemble	-	-	Araújo and New (2007)	0.85

P: Presence; A: Absence; B: Background.

entropy (MaxEnt), and random forest (RF). Machine learning algorithms directly generate the environmental space using input data. Classification algorithms such as classification and regression trees (CART) and flexible discriminate analyses (FDA) successively divide data into homogenous partitions. Surface range envelope (SRE), the only enveloping method used in this study, investigates environmental conditions at the points of occurrence and uses the results to find similar areas (Merow et al. 2014).

Variable importance was calculated by a permutation procedure used in biomod, which is independent of the modelling technique. Once the models were trained (i.e., calibrated), a standard prediction was made. Then, one of the variables was randomized and a new prediction was made. The correlation score between the new prediction and the standard prediction was calculated and gave an estimation of the variable importance in the models (Thuiller et al., 2009).

Models were evaluated using the True Skill Statistic (TSS). TSS is the sum of sensitivity and specificity minus 1, and does not depend on prevalence (Allouche et al. 2006; Fielding and Bell 1997). TSS was used to create an ensemble-forecasting framework, as per Araújo and New (2007). All models contributed to the ensemble model. However, those with better performance, as indicated by TSS, were given more weight (Thuiller et al. 2009). A threshold value was defined by maximizing training sensitivity and specificity in order to create a binary (presence/absence) map from outputs of the algorithms (Liu et al. 2005; Liu et al. 2011). Sensitivity and specificity are statistical index of the performance of a binary classification analysis. Sensitivity calculate the proportion of actual presences which are correctly predicted as such, while specificity calculate the proportion of pseudoabsences which are predicted as absences. By maximizing the sum of sensitivity and specificity, the associated threshold corresponds to the point on the ROC curve (i.e. sensitivity against 1-specificity) whose tangent slope is equal to 1 (Kaivanto 2008; Jiguet et al. 2011). The approach was selected to calculate the threshold for presence/absence predictions in biomod2 (Liu et al. 2005).

Presence data and environmental variables

Occurrence records and distribution of the species were obtained from herbariums of Ferdowsi University of Mashhad, Tehran University, and University of Birjand. Flora Iranica (Rechinger, 1963-2015) and Flora of Iran (Assadi et al. 1988-2017). Herbaria data were obtained from field samplings between 2009 and 2019. The coordinates of all the occurrence points were recorded using a hand-held multichannel Global Positioning System (GPS) receiver with a positional accuracy of ±5 m. The spatially correlated presence points were removed using spatial autocorrelation and Moran's I test. The number of presence points was 83 (Fig. 1).

Topographic, geographic, edaphic, and climatic variables were used as input for the algorithms. Topographic variables were obtained from the national cartographic center of Iran (NCC) at 1-km spatial resolution. Geological survey and mineral exploration of Iran (GSI) provided the geographic data at 1-km spatial resolution. Edaphic variables were accessed from the agricultural research, education and extension organization of Iran (AREEO) at 1-km spatial resolution.

Mean elevation and mean slope for all raster cells in a 1-km radius were the two topographic variables used in modeling. Geographic and edaphic variables included soil orders and lithology, respectively. An initial set of 20

Table 2. Environmental predictors and their relative contributions to ensemble model of *E. angustifolia*.

Environmental variables	Mean +SD	Relative contribution (%)
Climatic variables		
Mean Diurnal Range[1] (°C)	38.01±3.08	4.0
Temperature Seasonality[2]	8162.63±995.89	0.3
Mean Temperature of Warmest Quarter (°C)	27.26±4.49	22.3
Mean Temperature of Coldest Quarter (°C)	6.39±5.87	1.0
Annual Precipitation (mm)	208.13±140.89	0.1
Precipitation of Wettest Quarter (mm)	111.34±64.48	0.4
Precipitation of Driest Quarter (mm)	5.86±13.09	1.1
Annual solar radiation (kJ m^{-2} day^{-1})	10743.56±1906.88	10.2
Topographic variables		
Altitude (m)	1251.24±686.64	0.2
Slope (degree)	6.20±7.93	0.6
Geographic variable		
Lithology	557 classes	50.2
Edaphic variable		
Soil order	20 classes	8.5

[1] Mean of monthly (max temp - min temp).

[2] Standard deviation × 100.

climatic variables, including precipitation, temperature, and solar radiation were obtained from the Worldclim database (http://www.worldclim.org). Climatic variables were used at a resolution of 30” (~ 1km). The correlation between all pairs of variables was tested. If -0.7 > r > +0.7, one of the two variables was excluded from the input data. The correlation tests reduced the number of variables to 12, which were subsequently used to model habitat suitability (Tab. 2).

RESULTS

All ten models showed a relatively good performance predicting the distribution of Russian-olive (Tab. 1). The results of modeling evaluation based on the TSS values showed that the combination of models performed relatively better than each individual model. Moreover, a model evaluation test showed that ensemble model performed better than other distribution models. The distribution map obtained from the ensemble model has been presented in Fig. 1. Our results showed that most of the suitable habitats for Russian-olive are located in the north of Iran. Only 9.5 percent of the country was suitable to grow this species (Fig. 1).

Suitable habitats based for each province have been presented in a separate map (Fig. 2). North Khorasan had the highest, and Ilam and Bushehr had the lowest proportion of suitable habitats among all provinces (Fig. 2). The

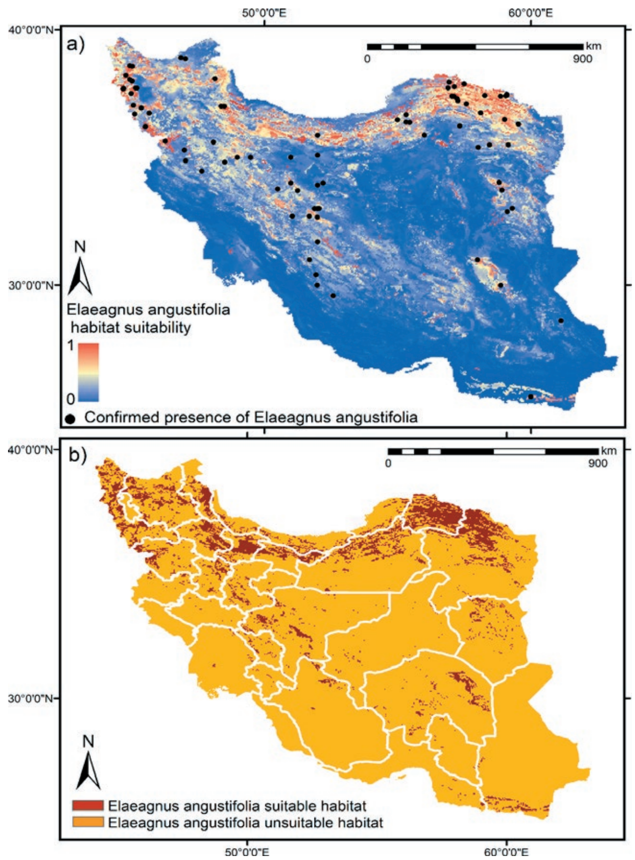

Fig. 1. Habitat suitability of *E. angustifolia* and its suitable habitats in Iran using ensemble model (a: continuous map, b: categorical map).

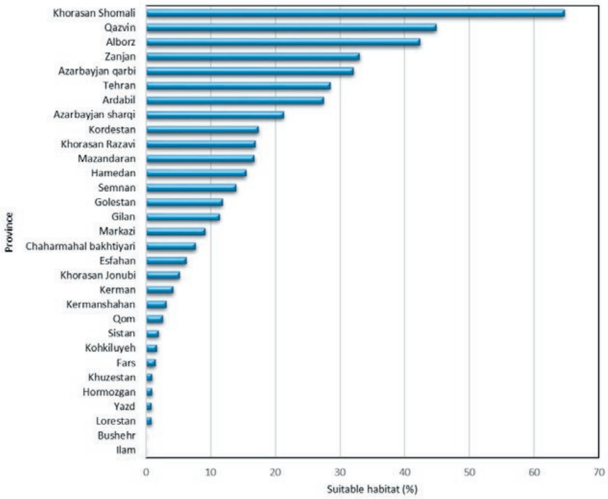

Fig. 2. Suitable habitats of *E. angustifolia* in each province.

relative importance of environmental variables changed based on different models. According to ensemble model, the most important environmental variables to predict habitat suitability for this species were lithology (50% of the contribution), mean temperature of the warmest quarter (22% of the contribution), annual solar radiation (10% of the contribution) and soil order (8% of the contribution) (Tab. 2).

Response curves for the four dominant environmental factors are shown in Fig. 3. There are unimodal relationships between habitat suitability and annual solar radiation. Peak presence probability was observed at 8150 kJ m^{-2} day^{-1}. The relationship between the habitat suitability values and mean temperature of the warmest quarter was best described by an exponential decay with the peak response at 5-7 °C. The results also demonstrated that any increase in mean temperature of the warmest quarter and

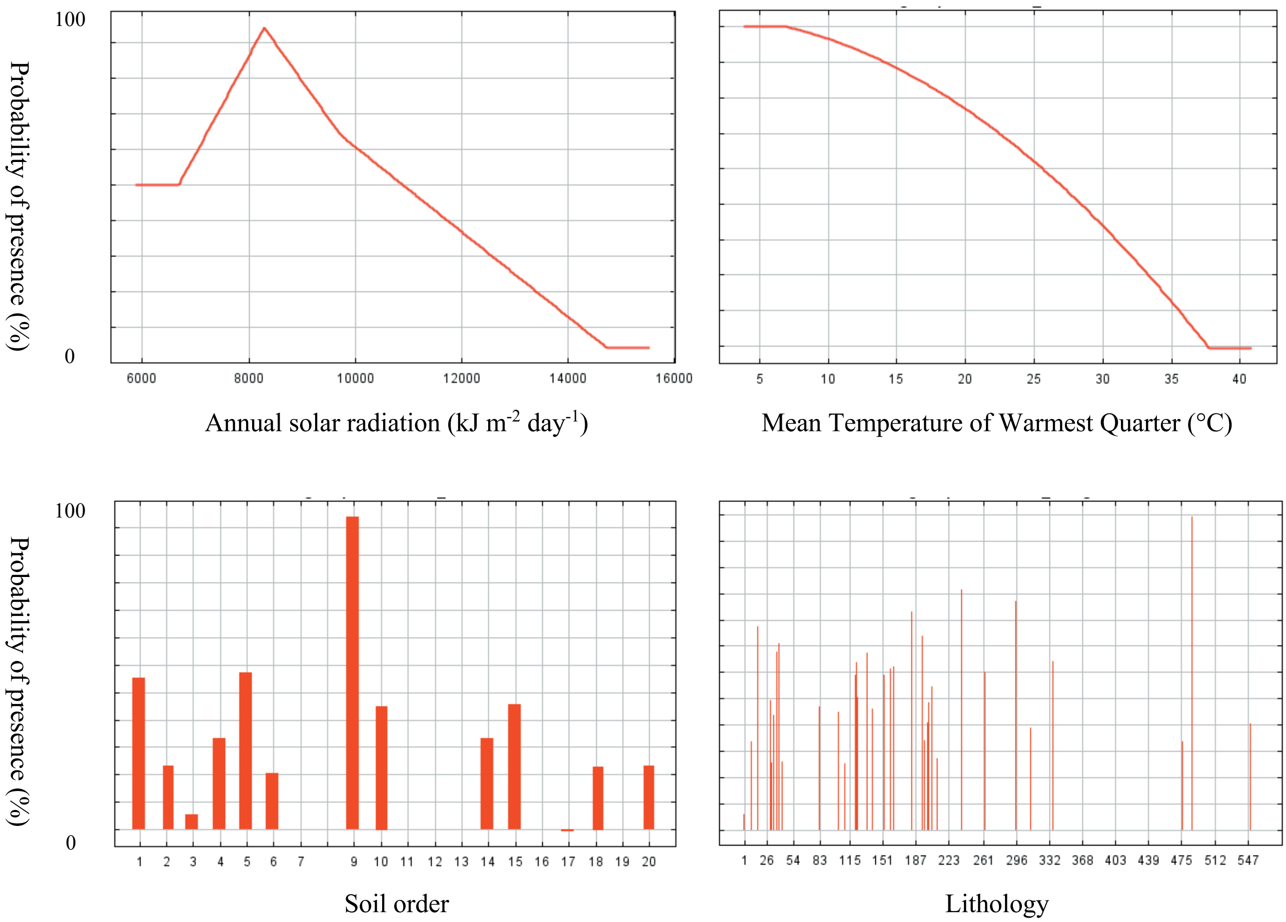

Fig. 3. Response curves of environmental variables for *E. angustifolia* (see soil order and lithology legend in supplementary file, Class 9 in soil order: rocky lands, Class 488 in lithology: high-level piedmont fan and valley terrace deposits).

annual solar radiation led to a decrease in habitat suitability for Russian-olive.

The relationship between the habitat suitability values with soil order and lithology showed that this species could grow in different soil and rock classes. However, the highest presence probability is observed in rocky lands and high-level piedmont fan and valley terrace deposits (Fig. 3).

DISCUSSION

Iran is a large country, containing a variety of climates. While the northern regions have a temperate climate, southern regions are dry and frequently experience droughts and water scarcity (Abbaspour et al., 2009; Bannayan et al., 2010). Our results show the prominent role of mean temperature of warmest quarter, annual solar radiation, lithology, and soil order in creating a suitable habitat for Russian-olive. The contribution of other variables was not considerable. Previous studies have shown that Russian-olive is capable of growing under both flooded and drought conditions in its native range (Asadiar, et al., 2013, Stannard et al., 2002) as well as its introduced range (Katz and Shafroth, 2003; Reynolds and Cooper, 2010). *E. angustifolia*'s extensive root network allows it to utilize moisture stored in deep soil or groundwater (Cui et al., 2015; Dubovyk et al., 2016). Owing to insufficient hydro-geological data, we could not use these variables in our study. Nevertheless, we recommend including them in future studies when they become available for Iran.

Our findings also reveal the importance of environmental variables such as soil (soil orders) and lithology in determining suitable habitats for Russian-olive, which supports the findings of previous studies (Zitzer and Dawson, 1992; Carman and Brotherson, 1982; Khamzina et al., 2009; Collette and Pither, 2015). The results demonstrate how Russian-olive can survive only under certain climatic conditions but can continue to grow on a number of soil orders and lithological formations (Lesica and Miles 2001; Katz and Shafroth, 2003; Reynolds and Cooper 2010; Collette and Pither, 2015). This makes Russian-olive a good candidate for shelterbelts in different regions (Olson and Knopf 1986; Pearce et al., 2009).

Roughly 9% of Iran is suitable habitat for Russian-olive, stretching along the Alborz and Koppeh-Dagh mountain ranges (Fig. 1). The Alborz and Koppeh-Dagh are comparable with temperate European mountain ranges such as the Alps in terms of endemism (Tribsch and Schonswetter 2003; Noroozi et al. 2008, 2018). Iranian provinces vary regarding habitat suitability for Russian-olive. All provinces, with the exception of Ilam and Bushehr (in the west and south of Iran, respectively), contained suitable habitats for Russian-olive. North Khorasan (64.7%), Qazvin (44.8%), and Alborz (42.4%) had the highest proportion of suitable habitats for Russian-olive. Suitability maps can inform future urban development and predict the future range of Russian-olive.

Therefore, it is suggested to protect the critical habitats of Russian-olive and use this species in urban green spaces. Russian-olive is not a demanding species and can survive for 50-80 years in different conditions. *E. angustifolia* is used to as a soil stabilizer, a hedge plant, and a fragrant ornamental. Due to its characteristics, Russian-olive is used in shelterbelts and urban landscapes (Kolesnikov, 1974; Kiseleva and Chindyaeva, 2011).

Russian-olive can become invasive (Reynolds and Cooper, 2010; Collette and Pither, 2015). After its introduction as an ornamental plant, Russian-olive became invasive in the US and Canada in the early 20th century (Katz and Shafroth 2003). The species negatively affected riparian forests and, as a result, was declared a noxious species in Colorado and New Mexico (Katz and Shafroth 2003; Collette and Pither, 2015). Introduction of this species to areas outside its native range should be done with caution. However, such considerations are not needed when planting Russian-olives in its native range since the species will not disrupt the natural processes of its native ecosystems (Strauss et al., 2006; Marsh-Matthews et al., 2011; Zhang et al., 2018). Moreover, native species can be advantageous to the local economy. As a result, we recommend the use of Russian-olive in urban landscapes in northern Iran.

A common assumption among SDMs is that species can only establish in areas that are ecologically similar to their native range (Kearney 2006). However, a species niche might change (Broennimann et al., 2007). As a result, the output of SDM algorithms is an approximation of species' niche in new environments. The differences in bioclimatic conditions between native areas and those we are making predictions for might lead to an underestimation of actual suitable areas. Thus, more accurate predictions can only be made by taking into account both biotic and abiotic variables and their interactions. These studies can be further improved through comparisons with areas under invasion by alien invasive species. In the meantime, the mere presence of suitable habitats for a species should not encourage managers to use the species before more extensive investigations are performed. However, the efficiency of SDMs is affected by several parameters (Allouche et al. 2008) such as the characteristics of environmental data (e.g. type, variance data; Aguirre-Gutiérrez et al. 2013), characteristics of species data (e.g. geographical accuracy, sample size, field survey constraints, or auto-correlation structure; Huettmann and Diamond 2006), species ecology (e.g. distribution range, abundance, niche limits of species; Saupe et al., 2012), computer power (i.e. too many cells may be too demanding on computer resources), model (e.g. presence only/presence-absence; Aguirre and Gutiérrez et al., 2013), and spatial resolution (Farashi and Naderi 2017). Despite their shortcomings, SDMs can still help us grasp the biological history of a species distribution (Silva Rocha et al., 2015). Further investigation is needed to study niche shift, distinguish the most influential variables, and pinpoint the role of other factors in determining distribution of the species.

ACKNOWLEDGMENT

This work was supported by Iran National Science Foundation [grant number 96002787].

REFERENCES

Abbas N, Wasimi S, Al-Ansari N, Sultana N 2018 Water resources problems of Iraq: Climate change adaptation and mitigation. Journal of Environmental Hydrology 26.

Abbaspour KC, Faramarzi M, Ghasemi SS, Yang H 2009 Assessing the impact of climate change on water resources in Iran. Water resources research 45(10).

Abreu-Harbich LV, Labaki LC, Matzarakis A 2015 Effect of tree planting design and tree species on human thermal comfort in the tropics. Landscape and Urban Planning 138: 99–109.

Aguirre-Gutiérrez, J., Carvalheiro, L. G., Polce, C., van Loon, E. E., Raes, N., Reemer, M., & Biesmeijer, J. C. (2013). Fit-for-purpose: species distribution model performance depends on evaluation criteria–Dutch hoverflies as a case study. PloS one, 8(5), e63708..

Akbolat D, Ertekin C, Menges HO, Guzel E, Ekinci K 2008 Physical and Nutritional Properties of Oleaster (*Elaeagnus angustifolia* L.) Growing in Turkey. Asian Journal of Chemistry 20(3): 2358-2366 Al-Ansari N, Abdellatif M, Zakaria S, Knutsson S, Mustafa Y 2014 Future Prospects for Macro Rainwater Harvesting (RWH) technique in north east Iraq. Journal of Water Resource and Protection 6(5): 403-420.

Al-Ansari N, Knutsson S 2011 Toward prudent management of water resources in Iraq. Journal of Advanced Science and Engineering Research (1): 53-67.

Allouche O, Tsoar A, Kadmon R 2006 Assessing the accuracy of species distribution models: prevalence, kappa and the true skill statistic (TSS). Journal of applied ecology 43(6): 1223-1232.

Allouche, O., Steinitz, O., Rotem, D., Rosenfeld, A., & Kadmon, R. (2008). Incorporating distance constraints into species distribution models. Journal of Applied Ecology, 45(2), 599-609..

Araújo, M.B. New, M 2007 Ensemble forecasting of species distributions. Trends in Ecology Evolution 22: 42–47.

Asadiar LS, Rahmani F, Siami A 2013 Assessment of genetic diversity in the Russian olive (*Elaeagnus angustifolia*) based on ISSR genetic markers. Revista Ciência Agronômica 44(2): 310-316.

Assadi M, Maassoumi AA, Khatamsaz M, Mozaffarian V. (Eds.) 1988–2017 Flora of Iran vols. 1–76 Research Institute of Forests and Rangelands Publications, Tehran .

Bannayan M, Sanjani S, Alizadeh A, Lotfabadi SS, Mohamadian A 2010 Association between climate indices, aridity index, and rainfed crop yield in northeast of Iran. Field Crops Research 118 (2): 105-114.

Bichai F, Ryan H, Fitzgerald C, Williams K, Abdelmoteleb A, Brotchie R, Komatsu R 2015 Understanding the role of alternative water supply in an urban water security strategy: An analytical framework for decision-making. Urban Water Journal 12(3): 175-189.

Broennimann O, Treier, UA, Müller-Schärer H, Thuiller W, Peterson AT, Guisan A 2007 Evidence of climatic niche shift during biological invasion. Ecology letters 10(8): 701-709.

Carman JG, Brotherson JD 1982. Comparisons of sites infested and not infested with saltcedar (*Tamarix pentandra*) and Russian olive (*Elaeagnus angustifolia*). Weed Science 30(4): 360-364.

Collette LK, Pither J 2015 Russian-olive (*Elaeagnus angustifolia*) biology and ecology and its potential to invade northern North American riparian ecosystems. Invasive Plant Science and Management 8(1): 1-14.

Cui Y, Ma J, Sun W, Sun J, Duan Z 2015 A preliminary study of water use strategy of desert plants in Dunhuang, China. Journal of Arid Land 7(1): 73-81.

Djuma H, Bruggeman, A, Eliades M Lange, M A 2016 Non-conventional water resources research in semi-arid countries of the Middle East. Desalination and Water Treatment 57(5): 2290-2303.

Dubovyk O, Menz G, Khamzina A 2016 Land suitability assessment for afforestation with *Elaeagnus angustifolia* L. In degraded agricultural areas of the lower amudarya river basin. Land Degradation Development 27(8): 1831-1839.

Elith J, Leathwick JR 2009 Species distribution models: ecological explanation and prediction across space and time. Annual review of ecology, evolution, and systematics 40: 677-697.

Farashi A, Alizadeh-Noughani M 2018 Effects of models and spatial resolutions on the species distribution model performance. Modeling Earth Systems and Environment 4(1): 263-268.

Farashi, A., & Naderi, M. (2017). Predicting invasion risk of raccoon Procyon lotor in Iran using environmental niche models. Landscape and Ecological Engineering, 13(2), 229-236..

Fielding AH, Bell JF 1997 A review of methods for the assessment of prediction errors in conservation presence/absence models. Environmental conservation 24(1): 38-49.

Ghahraman A, Attar F 2001 Biodiversity of plant species in Iran. Published by Tehran University, 1, pp. 1210.

Guida RJ, Abella SR, Smith Jr WJ, Stephen H, Roberts CL 2014 Climatic change and desert vegetation distribution: Assessing thirty years of change in southern Nevada's Mojave Desert. The Professional Geographer 66(2): 311-322.

Guisan A, Thuiller W 2005 Predicting species distribution: offering more than simple habitat models. Ecology letters 8(9): 993-1009.

Guisan A, Zimmermann NE 2000 Predictive habitat distribution models in ecology. Ecological modelling 135(2): 147-186.

Hannah L, Midgley G, Davies I, Davies F, Ries L, Thuiller W, Stoms D 2015 BioMove-Improvement and Parameterization of a Hybrid Model for the Assessment of Climate Change impacts on the Vegetation of California.

Haq SMA 2011 Urban green spaces and an integrative approach to sustainable environment. Journal of environmental protection 2(05): 601.

Haq SMA 2015 Urban green spaces and an integrative approach to sustainable environment. Urban Ecology: Strategies for Green Infrastructure and Land Use; Etingoff, K., Ed, 147-16.

Hemsing L, Bryn A 2012 Three methods for modelling potential natural vegetation (PNV) compared: A methodological case study from south-central Norway. Norsk Geografisk Tidsskrift-Norwegian. Journal of Geography 66(1): 11-29.

Hu Z, Guo K, Jin S Pan H 2018 The influence of climatic changes on distribution pattern of six typical *Kobresia* species in Tibetan Plateau based on MaxEnt model and geographic information system. Theoretical and Applied Climatology 1-16.

Huettmann, F., & Diamond, A. W. (2006). Large-scale effects on the spatial distribution of seabirds in the Northwest Atlantic. Landscape Ecology, 21(7), 1089-1108.

Jiguet, F., Barbet-Massin, M., & Chevallier, D. (2011). Predictive distribution models applied to satellite tracks: modelling the western African winter range of European migrant Black Storks Ciconia nigra. Journal of Ornithology, 152(1), 111-118..

Kaivanto, K. (2008). Maximization of the sum of sensitivity and specificity as a diagnostic cutpoint criterion. Journal of clinical epidemiology, 61, 516-518..

Karimi Afshar N, Karimian Z, Doostan R, Habibi Nokhandan M 2018 influence of planting designs on winter thermal comfort in an urban park. Journal of Environmental Engineering and Landscape Management 26(3): (232-240).

Katz GL, Shafroth PB 2003 Biology, ecology and management of *Elaeagnus angustifolia* L. (Russian olive) in western North America. Wetlands 23(4): 763-777.

Kearney M 2006 Habitat, environment and niche: what are we modelling? *Oikos* 115(1), 186-191.

Khamzina A, Lamers JP, Vlek PL 2009 Nitrogen fixation by *Elaeagnus angustifolia* in the reclamation of degraded croplands of Central Asia. Tree physiology 29(6): 799-808.

Kiseleva TI, Chindyaeva LN 2011 Biology of oleaster (*Elaeagnus angustifolia* L.) at the northeastern limit of its range. Contemporary Problems of Ecology 4(2): 218-222.

Klich MG 2000 Leaf variations in *Elaeagnus angustifolia* related to environmental heterogeneity. Environmental and Experimental Botany 44: 171–183.

Kolesnikov AI 1974 *Dekorativnaya dendrologiya* [Decorative dendrology]. Moscow: Lesnaya promyshlennost'[in Russian].

Kumar S, Stohlgren TJ. 2009 Maxent modeling for predicting suitable habitat for threatened and endangered tree *Canacomyrica monticola* in New Caledonia. Journal of Ecology and the Natural Environment 1(4): 94-98.

Lesica P, Miles S 2001 Natural history and invasion of Russian olive along eastern Montana rivers. *Western North American Naturalist*, 1-10.

Liang CT, Stohlgren TJ. 2011. Habitat suitability of patch types: A case study of the Yosemite toad. Frontiers of Earth Science, 5: 217-228.

Liang CT, Grasso RL, Nelson-Paul JJ, Vincent KE, Lind AJ 2017 Fine-Scale Habitat Characteristics Related to Occupancy of the Yosemite Toad, *Anaxyrus canorus*. Copeia 105(1): 120-127.

Liu C, Berry PM, Dawson TP, Pearson, RG 2005 Selecting thresholds of occurrence in the prediction of species distributions. Ecography, 28(3): 385-393..

Liu C, White M, Newell G 2011 Measuring and comparing the accuracy of species distribution models with presence–absence data. Ecography 34(2), 232-243.

Marsh-Matthews E, Matthews WJ, Franssen NR 2011 Can a highly invasive species re-invade its native community? The paradox of the red shiner. Biological Invasions 13(12): 2911-2924.

Merow C, Smith M., Edwards Jr TC, Guisan A, McMahon SM, Normand S, Elith J 2014 What do we gain from simplicity versus complexity in species distribution models? Ecography 37(12): 1267-1281.

Mikolajczak A, Maréchal D, Sanz T, Isenmann M, Thierion V, Luque S 2015 Modelling spatial distributions of alpine vegetation: A graph theory approach to delineate ecologically-consistent species assemblages. Ecological informatics 30: 196-202.

Modarres R, da Silva VDPR 2007 Rainfall trends in arid and semi-arid regions of Iran. Journal of arid environments 70(2): 344-355.

Noroozi J, Akhani H, Breckle SW 2008 Biodiversity and phytogeography of the alpine flora of Iran. Biodiversity and Conservation 17(3): 493-521.

Noroozi J, Talebi A, Doostmohammadi M, Rumpf SB, Linder HP, Schneeweiss GM 2018 Hotspots within a global biodiversity hotspot-areas of endemism are associated with high mountain ranges. Scientific reports 8.

Olson T E, Knopf FL 1986 Naturalization of Russian-olive in the western United States. Western Journal of Applied Forestry 1(3): 65-69.

Pearce CM, Smith DG, VanDevender TR, Espinosa-Garcia F., Harper-Lore BL, Hubbard T 2009 Rivers as conduits for long-distance dispersal of introduced weeds: example of Russian olive (*Elaeagnus angustifolia*) in the northern Great Plains of North America. Invasive Plants on the Move: Controlling Them in North America 410-427.

Peterson AT, Papes M, Kluz DA 2003 Predicting the potential invasive distributions of four alien plant species in North America. Weed Science 51(6): 863-868.

Rechinger KH, (ed.) 1963–2015 Flora Iranica, vols. 1–181. Akademische Druck- u. Verlagsanstalt, Graz; vol. 175. Akademische Verlagsgesellschaft, Salzburg; vols. 176–181. Verlag des Naturhistorischen Museums, Wien.

Reynolds LV, Cooper DJ 2010 Environmental tolerance of an invasive riparian tree and its potential for continued spread in the southwestern US. Journal of Vegetation Science 21(4): 733-743.

Rooper CN, Sigler MF, Goddard P, Malecha P, Towler R, Williams K, Zimmermann M 2016 Validation and improvement of species distribution models for structure-forming invertebrates in the eastern Bering Sea with an independent survey. Marine Ecology Progress Series 551: 117-130.

Saboonchian F, Jamei R, Sarghein SH 2014 Phenolic and flavonoid content of *Elaeagnus angustifolia* L. (leaf and flower). Avicenna journal of phytomedicine 4(4): 231.

Saupe, E. E., Barve, V., Myers, C. E., Soberón, J., Barve, N., Hensz, C. M., ... & Lira-Noriega, A. (2012). Variation in niche and distribution model performance: the need for a priori assessment of key causal factors. Ecological Modelling, 237, 11-22..

Silva Rocha I, Salvi D, Sillero N, Mateo JA, Carretero MA 2015 Snakes on the Balearic Islands: an invasion tale with implications for native biodiversity conservation. PloS one 10(4): e0121026.

Stannard M, Ogle D, Holzworth L, Scianna J, Suleaf E 2002 History, biology, ecology, suppression of Russian olive (*Elaeagnus angustifolia* L.). Boise, ID: USDA-NRCS 1-14.

Stratu A, Costică N, Costică M 2016 Wooden species in the urban green areas and their role in improving the quality of the environment. PESD 10(2): 173-184.

Strauss S., Webb CO, Salamin N 2006 Exotic taxa less related to native species are more invasive. Proceedings of the National Academy of Sciences 103(15): 5841-5845.

Thoma JK, Couttsa AM, Broadbenta AM, Tapper NJ 2016 The influence of increasing tree cover on mean radiant temperature across a mixed development suburb in Adelaide, Australia, Urban Forestry & Urban Greening 20: 233–242.

Thuiller W, Georges D, Engler R 2014 biomod2: Ensemble platform for species distribution modeling. 3:1-64.

Thuiller W., Lafourcade B., Engler R., Araújo M.B. 2009. BIOMOD–a platform for ensemble forecasting of species distributions. *Ecography* 32(3): 369-373. .

Tribsch A, Schönswetter P 2003 Patterns of endemism and comparative phylogeography confirm palaeo-environmental evidence for Pleistocene refugia in the Eastern Alps. Taxon 52(3): 477-497.

Willis AJ 2001 Endangered plants in Iran. New phytologist 149(2): 165-165.

Zhang X, Li G, Du S 2018 Simulating the potential distribution of *Elaeagnus angustifolia* L. based on climatic constraints in China. Ecological Engineering 113: 27-34.

Zhang X, Mi F, Lu N, Yan N, Kuglerova L, Yuan S, Ma OZ 2017 Green space water use and its impact on water resources in the capital region of China. Physics and Chemistry of the Earth, Parts A/B/C 101: 185-194.

Zhang ZD, Zang RG, Convertino M 2013 Predicting the distribution of potential natural vegetation based on species functional groups in fragmented and species-rich forests. Plant Ecology and Evolution 146(3): 261-271.

Zitzer SF, Dawson JO 1992 Soil properties and actinorhizal vegetation influence nodulation of *Alnus glutinosa* and *Elaeagnus angustifolia* by Frankia. Plant and Soil 140(2): 197-204.

Lithology legend

ID	Geo unit	Description
1	Ewf	Flysch with exotic blocks of Eocene limestone, Cretaceous limestone and ophiolitic components
2	gb	Gabbro
3	gb	Layered and isotropic gabbro
4	gsch	Glaucophane schist
5	h	Contact metamorphic rocks: two mica Hornfels; cordierite Hornfels; andalusite-sillimanite Hornfels and locally metamorphosed carbonate rocks
6	hz	Harzburgite
7	Island	Unknown
8	Ja.bv	Andesitic and basaltic volcanic rocks
9	Ja.bvt	Andesitic to basaltic volcanic tuff
10	Jav	Andesitic volcanic
11	Javs	Andesitic volcano sediment
12	Javt	Andesitic volcanic tuff
13	Jbash	Shale with intercalations of sandstone
14	Jbd	Dark grey, well-bedded, oolitic, ammonitiferous limestone, sandstone and shale
15	Jbg	Pale-green silty shale and sandstone
16	Jbv	Basaltic volcanic
17	am	Amphibolite
18	ba	Basalt and basaltic andesite pillow lavas
19	Cag	Grey thick-bedded to massive limestone and dolomite
20	Cb	Alternation of dolomite, limestone and verigated shale
21	Cd	Dolomite, quartzarenite, shale and limestone containing Trilobite
22	Cg	Limestone, shale, dolomite and gypsum
23	Cl	Dark red medium-grained arkosic to subarkosic sandstone and micaseous siltstone
24	Cm	Dark grey to black fossiliferous limestone with subordinate black shale
25	COm	Dolomite platy and flaggy limestone containing trilobite; sandstone and shale
26	Cs	Light olive-green shale with intercalations of quartzarenite and fossiliferous limestone
27	Cz	Dark red, micaceous siltstone and fine-grained sandstone
28	Czl	Undifferentiated unit, composed of dark red micaceous siltstone and sandstone
29	D2met	Alternation of marble, micaschist, amphibolite and quartzite
30	db	Diabase
31	Db	Grey and black, partly nodular limestone with intercalations of calcareous shale
32	Db-sh	Undifferentiated limestone, shale and marl
33	DC2met	Mica schist, green schist, graphite schist, and minor marble
34	DCkh	Yellowish, thin to thick-bedded, fossiliferous argillaceous limestone, dark grey limestone, greenish marl and shale, locally including gypsum
35	DCsh	Alternation of shale, marl and limestone
36	di-gb	Gabbro to diorite, diorite and trondhjemite
37	Dp	Light red to white, thick bedded quartzarenite with dolomite intercalations and gypsum
38	Ds	Black and grey dolomite
39	Dsb	Dolomite, limestone and shale
40	Dsh	Alternation of shale, marl and fossiliferous limestone, clay with intercalations of quartz arenite
41	du	Dunite
42	E	Undivided Eocene rocks
43	E1-2f	Lower-Middle Eocene flysch-sandstone, shale volcanoclastic sandstone, coarse grained siliceous sandstone minor limestone and pebble conglomerate
44	E1c	Pale-red, polygenic conglomerate and sandstone
45	E1f	Silty shale, sandstone, marl, sandy limestone, limestone and conglomerate
46	E1l	Nummulitic limestone
47	E1m	Marl, gypsiferous marl and limestone
48	E1s	Sandstone, conglomerate, marl and sandy limestone
49	E2-3f	Sandstone, calcareous sandstone and limestone
50	E2c	Conglomerate and sandstone
51	E2f	Sandstone, calcareous sandstone and limestone
52	E2l	Nummulitic limestone
53	E2m	Pale red marl, gypsiferous marl and limestone
54	E2mg	Gypsiferous marl
55	E2s	Sandstone, marl and limestone
56	E2sht	Tuffaceous shale and tuff
57	E3c	Conglomerate and sandstone
58	E3f	Sandstone-shale sequence with siltstone, mudstone, limestone and conglomerate
59	E3m	Marl, sandstone and limestone
60	E3sm	Sandstone and marl
61	Ea.bv	Andesitic and basaltic volcanic
62	Ea.bvs	Andesitic to basaltic volcano sediment
63	Ea.bvt	Andesitic to basaltic volcanic tuff
64	Eabvb	Andesitic to basaltic volcano breccia
65	Easv	Andesitic subvolcanic
66	Eat	Andesitic tuff
67	Eav	Unknown
68	Eav	Andesitic volcanic
69	Eavb	Andesitic volcano breccia
70	Eavs	Andesitic volcano sediment
71	Eavt	Andesitic volcanic tuff
72	Ebt	Basaltic tuff
73	Ebv	Basaltic volcanic rocks
74	Ebvs	Basaltic volcano sediment
75	Ebvt	Basaltic volcanic tuff
76	Ed.asv	Dacitic to andesitic subvolcanic rocks
77	Ed.at	Dacitic to Andesitic tuff
78	Ed.avb	Dacitic to Andesitic volcano breccia
79	Ed.avs	Dacitic to Andesitic volcano sediment
80	Edav	Dacitic to Andesitic volcanic

ID	Geo unit	Description
81	Edavt	Dacitic andesitic volcanic tuff
82	Edi	Diorite
83	Edsv	Rhyolitic to rhyodacitic subvolcanic
84	Edt	Rhyolitic to rhyodacitic tuff
85	Edv	Rhyolitic to rhyodacitic volcanic
86	Edvb	Rhyolitic to rhyodacitic volcano breccia
87	Edvs	Rhyolitic to rhyodacitic volcano sediment
88	Edvt	Rhyolitic to rhyodacitic volcanic tuff
89	Ef	Eocene flysch in general, composed of shale, marl, sandstone, conglomerate and limestone
90	Efv	Silty shale, marl, thin-bedded limestone, tuffaceous sandstone and basaltic volcanic rocks
91	Egb	Gabbro
92	Egr	Granite
93	Egr-di	Granite to diorite
94	Eja	Grey and brown weathered, massive dolomite, low weathered thin to medium -beded dolomite and massive, feature forming, buff dolomitic limestone
95	Ek	Well bedded green tuff and tuffaceous shale
96	Ek.a	Calcareous shale with subordinate tuff
97	Ekgy	Gypsum
98	Ekh	Olive-green shale and sandstone
99	Ekn	Tine-bedded argillaceous limestone and calcareous shale
100	Eksh	Greenish-black shale, partly tuffaceous with intercalations of tuff
101	Ekv1	Early-Eocene, sandstone, siltstone and shale with nummulitic limestone intercalation
102	Ekv2	Middle-Eocene, lower part composed of sandstone, siltstone and shale
103	Ekv3	Middle-Eocene, upper part composed of sandstone, siltstone shale and marl with limestone intercalation
104	EMas-sb	Undivided Asmari and Shahbazan Formation
105	EOa-bv	Andesitic to basaltic volcanic
106	EOas-ja	Undivided Asmari and Jahrum Formation, regardless to the disconformity separates them
107	EOasv	Eocene-Oligocene andesitic subvolcanic
108	EOav	Eocene-Oligocene andesitic lava flows
109	EObv	Eocene-Oligocene basaltic lava flows
110	EOd	Eocene-Oligocene diorite
111	EOd-av	Dacitic to Andesitic volcanic
112	EOdsv	Eocene-Oligocene rhyolitic to rhyodacitic subvolcanic
113	EOdv	Rhyolitic to rhyodacitic volcanic rocks
114	EOf	Rytmically bedded sandstone and shale with volcanoclastic sandstone, minor limestone and tuff
115	EOgr	Eocene-Oligocene granite and granodiorite
116	EOgr-d	Eocene-Oligocene granite to diorite
117	EOgy	Gypsum
118	EOsa	Salt dome
119	EOsc	Sandstone, siltstone, shale and conglomerate
120	EOt	Ignembrite and tuff
121	Eph	Phyllite

ID	Geo unit	Description
122	Esl	Red shale and pelagic limestone
123	Eslv	Red shale, pelagic limestone and amigdaloidal basic volcanic rocks
124	Jch	Dark grey argillaceous limestone and marl
125	Jd	Well-bedded to thin-bedded, greenish-grey argillaceous limestone with intercalations of calcareous shale
126	Jd.avs	Dacitic to Andesitic volcano sediment
127	Jdav	Jurassic dacite to andesite lava flows
128	Jdt	Rhyolitic to rhyodacitic tuff
129	Jdvt	Rhyolitic to rhyodacitic volcanic tuff
130	Je	Massive, light-grey reef limestone
131	Jel	Reefal limestone
132	Jf	Flysch turbidites sandstone, shale, conglomerate, volcanic rocks and limestone; this unit transgresivly overlies the metamorphic rocks
133	Jh	Alternation of sandstone and sandy to argillaceous shale with intercalations of coal and carbonaceous shale
134	Jk	Conglomerate, sandstone and shale with plantremains and coal seams
135	JKav	Andesitic flows and their associated pyroclastics with or without intercalations of limestone
136	JKbl	Grey, thick-bedded, oolitic, fetid limestone
137	Jkc	Honogenous, well rounded quartzos conglomerate
138	JKdi	Diorite
139	JKkgp	Undivided Khami Group, consist of massive thin-bedded limestone comprising the following formations: Surmeh, Hith Anhydrite, Fahlian, Gadvan and Dariyan
140	JKkgp-bgp	Jurassic to Cretaceous undivided sedimentary rocks including Khami and Bagestan Groups
141	JKl	Crystalized limestone and calc- schist
142	Jks	Alternation of sandstone and shale
143	JKsj	Pale red argillaceous limestone, marl, gypsiferous marl, sandstone and conglomerate
144	Jl	Light grey, thin-bedded to massive limestone
145	Jmz	Grey thick-bedded limestone and dolomite
146	Jph	Phyllite, slate and meta-sandstone (Hamadan Phyllites)
147	Jq	Sandstone, shale, thin-bedded limestone and calcareous shale
148	Jr	Red manganiferous chert
149	Js	Shale with intercalations of conglomerate, sandstone, radiolarite, limestone and volcanic
150	Jsc	Conglomerate
151	Jshl.s	Sandy to silty gluconitic limestone and calcareous limestone
152	Jsm	Thick-bedded to massive dolomitic limestone, thin-bedded argillaceous limestone and marl
153	Jss	Sandstone
154	JUavs	Andesitic volcano sediment
155	JUavt	Andesitic volcanic Tuff

ID	Geo unit	Description
156	Jub	Sandstone, siltstone, Pectinid limestone, marl, gypsum
157	Juc	White, quartzous conglomerate
158	Judi	Upper Jurassic diorite
159	JUdv	Rhyolitic to rhyodacitic volcanic
160	Jugn	Granite gneiss normally with augen structure
161	Jugr	Upper Jurassic granite including Shir Kuh Granite and Shah Kuh Granite
162	Jugr	Upper Jurassic granite including Shir Kuh Granite and Shahkuh Granite
163	Jugr-di	Upper Jurassic granite to diorite intrusive
164	Jugy	Gypsum
165	Jumb	Late Jurassic marble and mamorized limestone
166	Jupl	Pectinid limestone and marl
167	Jurb	Sandstone, siltstone, and fine-grained conglomerate
168	Jus	Red sandstone and siltstone
169	K	Cretaceous rocks
170	K1-2lm	Albian-Cenomanian marl and argillaceous limestone
171	K1a.bv	Andesitic and basaltic volcanic rocks
172	K1avt	Andesitic volcanic tuff
173	K1bl	Grey, thick-bedded to massive oolitic limestone
174	K1bv	Early-Cretaceous basaltic lava flows
175	K1bvt	Basaltic volcanic tuff
176	K1c	Red conglomerate and sandstone
177	K1l	Massive to thick-bedded orbitolina limestone
178	K1m	Limestone, argillaceous limestone; tile red sandstone and gypsiferous marl
179	K2a.bv	Andesitic and basaltic volcanic rocks
180	K2asv	Andesitic subvolcanic
181	K2av	Andesitic volcanic
182	K2bv	Basaltic volcanic
183	K2c	Conglomerate and sandstone
184	K2d.asv	Dacitic to andesitic subvolcanic rocks
185	K2d.av	Dacitic to Andesitic volcanic
186	K2di	Diorite
187	K2gb	Gabbro
188	K2gr	Granite
189	K2l	Hyporite bearing limestone
190	K2l,m,s	Limestone, marl and sandstone
191	K2l1	Hyporite bearing limestone
192	K2l2	Thick-bedded to massive limestone
193	K2lm	Pale-red marl, gypsiferous marl and limestone
194	K2m,l	Marl, shale and detritic limestone
195	K2shm	Shale calcareous shale and sandstone with intercalations of limestone
196	Ka.bv	Andesitic to basaltic volcanic
197	Kab	Blue-grey marl and shale
198	M1f	Rhytmically bedded sandstone, calcareous sandstone, mudstone, gypsiferous mudstone and shale
199	M2-3s	Sandstone, siltstone, conglomerate, shale, mudstone and shell beds
200	M2gm	Gypsiferous and calcareous marl, marlstone and mudstone with interbedded siltstone and sandstone (Gushi Marl and part of Sabz unit)
201	M3ms	Marl and marlstone, locally gypsiferous and sandstone with interbedded shale and marl
202	Ma.bv	Andesitic-basaltic volcanic rocks
203	Mat	Andesitic tuff
204	Mav	Miocene andesitic lava flows locally basalt
205	mb	Marble
206	Mbv	Basaltic volcanic rocks
207	Mc	Red conglomerate and sandstone
208	Mcs	Red conglomerate, sandstone, siltstone and mudstone
209	Md.av	Dacitic to andesitic subvolcanic rocks
210	Mdt	Rhyolitic to rhyodacitic tuff
211	Mgr	Granite
212	Mgs	Anhydrite, salt, grey and red marl alternating with anhydrite, argillaceous limestone and limestone
213	Mm,s,l	Marl, calcareous sandstone, sandy limestone and minor conglomerate
214	Mmn	Unknown
215	Mmn	Low weathering gray marls alternating with bands of more resistant shelly limestone
216	Mms	Alternations of marl, silty clay shale, sandstone and dolomitic limestone
217	MPa.bv	Andesitic to basaltic volcanic
218	MPa.bvt	Andesitic to basaltic volcanic tuff
219	MPasv	Andesitic subvolcanic
220	MPd.av	Dacitic to andesitic volcanic
221	MPLav	Andesitic volcanic
222	MPlc	Polymictic conglomerate, sandstone and mudstone
223	MPLdvt	Rhyolitic to rhyodacitic volcanic tuff
224	MPlfgp	FARS GROUP comprising the following formation Gachsaran, Mishan and Aghajari,
225	MPls	sandstone with siltstone, mudstone and minor conglomerate
226	Ms	Sandstone siltstone with minor conglomerate
227	Msc	Varigated gypsiferous clay shale; conglomerate and sandstone
228	MuPlaj	Brown to grey, calcareous, feature-forming sandstone and low weathering, gypsum- veined, red marl and siltstone
229	Mur	Red marl, gypsiferous marl, sandstone and conglomerate
230	Murc	Red conglomerate and sandstone
231	Murgy	Gypsum
232	Murm	Light-red to brown marl and gypsiferous marl with sandstone intercalations
233	Murmg	Gypsiferous marl
234	Mursh	Varigated shale, gypsiferous marl and sandstone
235	Mv	Volcanic in general
236	Mvs	Tuff interbedded with sandstone and siltstone
237	Oa.bv	Andesitic to basaltic volcanic

ID	Geo unit	Description
238	Oa.bvs	Andesitic to basaltic volcano sediment
239	Oasv	Andesitic subvolcanic
240	Oat	Andesitic tuff
241	Oav	Oligocene andesitic lava flows
242	Oavt	Andesitic volcanic tuff
243	Obv	Basaltic Volcanic
244	Oc	Polimictic conglomerate, sandstone and siltstone
245	Od.asv	Dacitic to andesitic subvolcanic rocks
246	Od.av	Dacitic to andesitic volcanic
247	Odi	Diorite
248	Odi-gb	Diorite to gabbro
249	Odsv	Rhyolitic to rhyodacitic subvolcanic
250	Odv	Rhyolitic to rhyodacitic volcanic
251	Odvb	Rhyolitic to rhyodacitic volcano breccia
252	Odvs	Rhyolitic to rhyodacitic volcano sediment
253	Odvt	Rhyolitic to rhyodacitic volcanic tuff
254	Ogb	Gabbro
255	Ogr	Granite
256	Ogr-di	Granite to diorite
257	Ogrsv	Granite subvolcanic
258	Olav	Rhyolitic to rhyodacitic volcanic rocks
259	Olc,s	Conglomerate and sandstone
260	Olgr	Oligocene granite and granodiorite
261	Olgy	Gypsum
262	Olm,s,c	Red and green silty, gypsiferous marl, sandstone and gypsum
263	om1	Tectonized association of peridotites, gabbro, diorite, trondhjemite, diabase and basic volcanic
264	om2	Tectonized association of pelagic limestone, radiolarian chert, radiolarian shale with basic volcanic and intrusive rocks of ophiolitic rocks
265	om3	Pelagic limestone, radiolarian chert and shale in association with basalt and basaltic andesite pillow lava
266	OMa.bv	Andesite and andesitic lava flow
267	OMap	Andesitic pyroclastic rocks
268	OMas	Cream to brown-weathering, feature-forming, well-jointed limestone with intercalations of shale
269	OMat	Andesitic tuff
270	OMav	Andesitic volcanic
271	OMavs	Andesitic volcano sediment
272	OMbt	Basaltic tuff
273	OMbv	Basalt and subvolcanic
274	OMbvb	Basaltic volcano breccia
275	OMbvs	Basaltic volcano sediment
276	OMc	Basal conglomerate and sandstone
277	OMd.at	Dacitic Andesitic tuff
278	OMd.av	Dacitic Andesitic volcanic
279	OMdi	Diorite
280	OMdi-gb	Diorite to gabbro
281	OMdsv	Rhyolitic to rhyodacitic subvolcanic
282	OMdv	Rhyolite and rhyodacite

ID	Geo unit	Description
283	OMdvs	Rhyolitic to rhyodacitic volcano sediment
284	OMdvt	Rhyolitic to rhyodacitic volcanic tuff
285	OMf	Rhytmically bedded sandstone and shale, with minor siltstone and mudstone
286	OMgb	Oligo-Miocene gabbro and microgabbro
287	OMgr	Oligo-Miocene granite and granodiorite
288	OMgr-di	Granite to diorite
289	OMl	Unknown
290	OMq	Limestone, marl, gypsiferous marl, sandymarl and sandstone
291	OMql	Massive to thick-bedded reefal limestone
292	OMqm	Marl with intercalations of limestone
293	OMr	Red, grey, and green silty marls interbedded with subordinate silty limestone and minor sandstone ribs
294	OMrb	Red Beds composed of red conglomerate, sandstone, marl, gypsiferous marl and gypsum
295	OMssh	Yellow-green shale and sandstone locally with limestone intercalation
296	OMz1	Alternation of varigated siltyclay shale with sandstone
297	OMz2	Massive to thick bedded tuffaceous sandstone and varigated shale
298	OMz3	Alternation of sandstone with siltstone and claystone
299	OPLavs	Andesitic volcano sediment
300	OS	Undifferentiated Ordivician and Silurian rocks
301	P34	Unknown
302	P	Undifferentiated Permian rocks
303	PAav	Andesitic volcanic
304	PAbv	Basaltic volcanic
305	PAbvt	Basaltic volcanic Tuff
306	PAdv	Rhyolitic to rhyodacitic volcanic
307	PAEa.bv	Andesitic to basaltic volcanic
308	PAEa.bvt	Andesitic to basaltic volcanic tuff
309	PAEav	Andesitic volcanic
310	PAEavb	Andesitic volcano breccia
311	PAEavs	Andesitic volcano sediment
312	PAEavt	Andesitic volcanic tuff
313	PAEbvs	Basaltic volcano sediment
314	PAgr	Granite
315	PAgr-di	Granite to diorite
316	pC-C	Late proterozoic-early Cambrian undifferentialed rocks
317	pC-Cd	Recrystalised dolomite and fetid limestone; violet-red micaceous sandstone and siltstone; gypsum
318	pC-Ch	Rock salt, gypsum & blocks of contorted masses of sedimentary material such as black laminated fetid limestone, brown cherty dolomite, red sandstone & varigated shale in association with igneous rocks such as diabase, basalt, rhyolite and trachyte
319	pC-Cs	Thick dolomite and limestone unit, portly cherty with thick shale intercalations
320	pCa.bv	Andesite and basalt
321	pCam	Amphibolite

ID	Geo unit	Description
322	pCav	Andesitic volcanic
323	pCbr	Dolomite and sandstone
324	pCdi	Precambrian diorite
325	pCdv	Rhyolitic to rhyodacitic volcanic
326	pCgn	Gneiss, granite gneiss and locally including migmatite
327	pCgr	Precambrian granite to granodiorite
328	pCgr-di	Granite to diorite
329	pCk	Dull green grey slaty shales with subordinate intercalation of quartzitic sandstone
330	pCmb	Marble
331	pCmt1	Medium-grade, regional metamorphic rocks
332	pCmt2	Low-grade, regional metamorphic rocks
333	pCph	Phyllite
334	pCr	Dolomite and limestone, partly cherty; redish sandy shale and sandstone, volcanic rocks and tuffs
335	pCrr	Acidic volcanic rocks
336	pd	Peridotite including harzburgite, dunite, lerzolite and websterite
337	Pd	Red sandstone and shale with subordinate sandy limestone
338	pd1	Ulttrabasic rocks
339	Pda	Limestone, dolomite, dolomitic limestone and thick layers of anhydrite in alternation with dolomite in middle part
340	Peasv	Andesitic subvolcanic
341	Pec	Conglomerate and sandstone
342	PeEck	Limestone, marl and gysiferous marl
343	PeEck-kh	Undifferentiated unit, including limestone, marl shale and sandstone
344	PeEf	Flysch turbidite, sandstone and calcareous mudstone
345	PeEm	Marl and gypsiferous marl locally gypsiferous mudstone
346	PeEpd	Blue and purple shale and marl interbedded with the argillaceous limestone
347	PeEph	Phyllite
348	PeEps-ck	Undifferentiated unit, including conglomerate, sandstone, limestone and marl
349	PeEs	Arkosic to subarkosic sandstone
350	PeEsa	Pale red marl, marlstone, limestone, gypsum and dolomite
351	PeEsh	Shale and calcareous shale
352	PeEtz	Grey and brown, medium-bedded to massive fossiliferous limestone
353	PeEz	Reef-type limestone and gypsiferous marl
354	Pel	Medium to thick-bedded limestone
355	Pem	Marl, gypsiferous marl and limestone
356	Pems	Mudstone calcareous shale, limestone and minor sandstone
357	Peps	Red well consolidated conglomerate, sandstone and mudstone
358	Pes	Sandstone, calcareous shale and mudstone

ID	Geo unit	Description
359	Pgf	Polygenic conglomerate, red sandstone and sandy mudstone
360	Pgkc	Light-red coarse grained, polygenic conglomerate with sandstone intercalations
361	pgr	Plagiogranite
362	Pj	Massive to thick-bedded, dark-grey, partly reef type limestone and a thick yellow dolomite band in the upper part
363	Pla.bv	Andesitic to basaltic volcanic
364	Plasv	Pliocene andesitic subvolcanic
365	Plat	Andesitic tuff
366	Plav	Andesitic lavas with minor basaltic andesite, tuff and breccias interbedded with volcanoclastic sandstone and boulder conglomerate (Bazman Volcanism)
367	Plbk	Alternating hard of consolidated, massive, feature forming conglomerate and low -weathering cross -bedded sandstone
368	Plbv	Basaltic lava flows
369	Plc	Polymictic conglomerate and sandstone
370	Plc	Polymictic conglomerate and sandstone
371	Pld.asv	Dacitic to andesitic subvolcanic rocks
372	Pld.at	Dacitic andesitic tuff
373	Pld.av	Dacitic andesitic volcanic
374	Pld.avs	Dacitic andesitic volcano sediment
375	Pldsv	Pliocene rhyolitic to rhyodacitic subvolcanic
376	Pldt	Rhyolitic to rhyodacitic tuff
377	Pldv	Rhyolitic to rhyodacitic volcanic
378	Pldvt	Rhyolitic to rhyodacitic volcanic tuff
379	Plgr	Granite
380	Plgr-di	Granite to diorite
381	Plmb1	Pyroclastics and claystone with vertebrate fauna remains
382	Plmb2	Ash flows and associated rocks
383	Plmb3	Ash flows and associated pyroclastic rocks, conglomerate, sandstone and shale
384	Plms	Marl, shale, sandstone and conglomerate
385	PlQabv	Andesite, andesitic basalt and olivine basalt
386	PlQap	Silty clay, sand, gravel and volcanic ash
387	PlQav	Andesitic volcanic
388	PlQavs	Andesitic volcanic in association with sedimentary rocks
389	PlQbv	Basaltic volcanic
390	PlQc	Fluvial conglomerate, Piedmont conglomerate and sandstone.
391	PlQd.avt	Dacitic andesitic volcanic tuff
392	PlQdv	Rhyolitic to rhyodacitic volcanic
393	PlQlu	Unfolded, poorly consolidated, yellowish silt, sand and gravel
394	PlQm	Lacustrine terraces fine grained deposits and lake sediments
395	PlQms	Poorly cemented, unindurated sandstone and mudstone
396	Pmb	Marble

ID	Geo unit	Description
397	Pml	Slightly metamorphosed fossiliferous (Fusulinid) limestone, locally crystaline limestone
398	Pn	Dark grey limestone and shale
399	Pr	Dark grey medium-bedded to massive limestone
400	Psch1	Metamorphosed turbidite including phyllite, crystaline limestone calc-schist
401	Psch2	Metamorphosed turbidite in associated with met ultrabasic and basic rock
402	PTR	Undifferentiated Permo-Triassic sedimentary rocks
403	px	Pyroxenite
404	Pz	Undifferentiated lower Paleozoic rocks
405	Pz1a.bv	Andesitic basaltic volcanic
406	Pz1av	Andesitic volcanic
407	Pz1di	Lower Paleozoic diorite
408	Pz1gn	Gneiss and anatectic granite
409	Qft1	High level piedmont fan and valley terrace deposits
410	TRml	Meta- limestone, meta-quartzarenite, phyllite and meta- volcanic
411	Pz2	Undifferentiated Upper Paleozoic rocks
412	PZ2a.bv	Andesitic basaltic volcanic
413	PZ2asv	Andesitic subvolcanic
414	PZ2bv	Basaltic volcanic
415	PZ2bvt	Basaltic volcanic tuff
416	PZ2gr	Granite
417	Pzkb	Undifferentiated basic schist pelitic schist, psammitic schist, calc-silicate rocks, amphibolite, recrystalized limestone, marble and phyllite
418	Qabv	Andesite to basaltic volcanic
419	Qabvs	Andesitic to basaltic volcano sediment
420	Qal	Stream channel, braided channel and flood plain deposits
421	Qasv	Andesitic subvolcanic
422	Qat	Andesitic tuff
423	Qav	Andesitic volcanic Basaltic volcanic
424	Qavs	Andesitic volcano sediment
425	Qba	Silty clay, sandy tuff and fresh water limestone
426	Qbv	Olivine basalt and basalt related to Bazman Volcanism and partly related to Taftan Volcanism
427	Qbvs	Basaltic volcano sediment
428	Qcf	Clay flat
429	Qcsm	Clay salt marsh
430	Qcu	Cultivated area
431	Qdi	Diorite
432	Qdt	Rhyolitic to rhyodacitic tuff
433	Pz1gr	Lower Paleozoic granite, including Zarigan granite and Narigan granite
434	Pz1mt	Gneiss, anatectic granite, amphibolite, kyanite, staurolite schist, quartzite and minor marble
435	Qft1	High level piedmont fan and valley terrace deposits
436	Qft1	High level piedmont fan and valley terrace deposits
437	Qft2	Low level piedmont fan and valley terrace deposits
438	Qft2	Low level piedmont fan and valley terrace deposits

ID	Geo unit	Description
439	Qft2	Low level piedmont fan and valley terrace deposits
440	Qft2	Low level piedmont fan and valley terrace deposits
441	Qft2	Low level piedmont fan and valley terrace deposits
442	Qft2	Low level piedmont fan and valley terrace deposits
443	Qft2	Low level piedmont fan and valley terrace deposits
444	Qft2	Low level piedmont fan and valley terrace deposits
445	Qft2	Low level piedmont fan and valley terrace deposits
446	Qft2	Low level piedmont fan and valley terrace deposits
447	Qft2	Low level piedmont fan and valley terrace deposits
448	Qgb	Gabbro
449	Qgr	Granite
450	Qitd	Intertidal deposits
451	Qm	Swamp and marsh
452	Qmt	Undifferentiated marine terraces
453	QPLavt	Andesitic volcanic tuff
454	QPLdasv	Dacitic to andesitic subvolcanic rocks
455	Qs	Sand dunes and sand sheet
456	Qs,d	Unconsolidated wind-blown sand deposit including sand dunes
457	Qsf	Salt flat
458	Qsl	Salt Lake
459	Qsw	Swamp
460	Qtr	Teravertine
461	Qvc	Coarse grained fanglomerate composed of volcaniclastic materials locally with intercalation of lava flows
462	sea	Unknown
463	sm1	Sedimentary melange-sheared and boudined sediments with no recognizable stratigraphy containing tectonic blocks of Cretaceous to Eocene age
464	sm2	Sedimentary melange-sheard and boudined sediments with norecognisable stratigraphy, containing tectonic blocks of Cretaseous to Miocene age
465	Sn	Greenish grey, shale, sandstone, sandylime, coral limestone and dolomite
466	sp	Spilitic rocks locally with pillow structure
467	sp1	Spilite spilitic andesite and diabasic tuff
468	spr	Sub-marine, vesicular basalt, locally with pillow structure in association with radiolarian chert
469	sr	Serpentinite
470	tm	Tectonic melange-association of ophiolitic components, pelagic limestone, radiolarian chert and shale with or without Eocene sedimentary rocks
471	TRa.bv	Triassic, andesitic and basaltic volcanic
472	TRav	Andesitic Volcanic
473	TRavt	Andesitic volcanic tuff
474	TRba	Red to light green conglomerate and microconglomerate with intercalations of sandstone and shale
475	TRbv	Basaltic volcanic
476	TRdl	Crystaline limestone and dolomite

ID	Geo unit	Description
477	TRe	thick bedded grey oolitic limestone; thin-platy, yellow to pinkish shaly limestone with worm tracks and well to thick-bedded dolomite and dolomitic limestone
478	TRe1	Thin bedded, yellow to pinkish argillaceous limestone with worm tracks
479	TRe2	Thick bedded dolomite
480	TRJa.bv	Andesitic to Basaltic Volcanic
481	TRJlr	Grey, thin to thick bedded, partly cherty, neritic limestone intercalation of radiolarian shale and chert
482	TRJs	Dark grey shale and sandstone
483	TRJvm	Meta-volcanic, phyllites, slate and meta- limestone
484	TRkk-nz	Thin to medium-bedded, dark grey dolomite; thin-bedded dolomite, greenish shale and thin-bedded argillaceous limestone
485	TRKubl	Kuh Bistoon limestone
486	TRKurl	Purple and red thin-bedded radiolarian chert with intercalations of neritic and pelagic limestone
487	TRmi	Shale and sandstone with coal seams
488	Qft1	High level piedmont fan and valley terrace deposits
489	TRn	Sandstone, quartz arenite, shale and fossiliferous limestone
490	TRn1	Grey green shale, siltstone and feldspathic sandstone underlain by pisolitic iron laterite horison
491	TRn2	Shale, Heterastridum bearing limestone and reddish-brown sandstone
492	TRn3	Shale interbedded with thin sandstone beds
493	TRn4	Black limestone, shale and sandstone
494	TRn5	Shale, siltstone, sandstone and thin sandy limestone with thin coal seams
495	TRqa	Red to brown shale, sandstone and conglomerate
496	TRs	Calcareous red shale
497	TRsh	Well-bedded, dense, yellow dolomite
498	TRsi	Tuffaceous sandstone, tuffaceous shale with intercalations of limestone, marl and conglomerate
499	TRuJm	Transitional zone composed of phyllite with intercalations of crystalized limestone and acidic volcanic horizons
500	Kad	White-cream Inoceramus bearing cherty and glauconitic argillaceous limestone
501	Kad-ab	Undifferentiated unit including argillaceous limestone, marl and shale
502	Kat	Olive green glauconitic sandstone and shale
503	Kav	Andesitic volcanic
504	Kavt	Andesitic volcanic tuff
505	Kbgp	Undivided Bangestan Group, mainly limestone and shale, Albian to Companian, comprising the following formations: Kazhdumi, Sarvak, Surgah and Ilam
506	Kbsh	Dark grey slightly phyllitized shale with intercalations of sandstone and limestone
507	Kbv	Basaltic volcanic
508	Kbvt	Basaltic volcanic tuff
509	Kd.av	Dacitic to Andesitic volcanic

ID	Geo unit	Description
510	Kda-fa	Grey to brown, partly oolitic, massive limestone; limestone in alternation with marl and thick-bedded to massive orbitolina bearing limestone
511	Kdi	Diorite
512	Kdzsh	Marl, shale, sandstone and limestone
513	KEpd-gu	Grey and brown, medium-bedded to massive fossiliferous limestone
514	Kfsh	Dark grey argillaceous shale
515	Kgb	Gabbro
516	Kgr	Granite
517	Kgu	Bluish grey marl and shale with subordinate thin-bedded argillaceous -limestone
518	Kk	Buff, thick-bedded limestone, marlstone and marl
519	Kkz	Grey to dark grey bituminous shale with intercations of limestone
520	Kl	Lower Cretaceous undifferentiated rocks
521	Klav	Andesitic volcanic rocks
522	Klsm	Marl, shale, sandy limestone and sandy dolomite
523	Klsol	Grey thick-bedded to massive orbitolina limestone
524	Knl	Massive grey to black limestone
525	Kns	Red sandstone and conglomeratic sandstone
526	Knsh	Dark green calcareous shale
527	Knz	Gloconitic sandstone
528	KPAavs	Andesitic Volcano sediment
529	KPeam	Dark olive-brown, low weathered siltstone and sandstone with local development of chert conglomerates and shelly limestone
530	KPedu	Undifferentiated limestone, basic to intermediate lava and pillow lava, metavolcanic, phyllite, schist, sediments, metasediments with minor tuff and intrusive rocks
531	KPef	Thinly bedded sandstone and shale with siltstone, mudstone limestone and conglomerate
532	KPefv	Crystal tuff, tuffaceous sandstone, recrystalized limestone and sandy limestone, red chert and pillow lava
533	KPegr	Late Cretaceous-Early Paleocene granite
534	KPegr-di	Late Cretaceous-Early Paleocene granite to diorite intrusive rocks
535	KPeph	Phyllite
536	KPvs	Volcanic and volcanoclastic rocks including tuff, basalt, minor conglomerate and slamp breccia
537	Ksm,l	Marl and calcareous shale with intercalations of limestone
538	Ksn	Grey to block shale and thin layers of siltstone and sandstone
539	Ksr	Ammonite bearing shale with interaction of orbitolin limestone
540	Ksv	Grey, thick-bedded to massive limestone with thin marl intercalations in upper part
541	Ktb	Massive, shelly, cliff-forming partly anhydritic limestone

ID	Geo unit	Description
542	Ktl	Thin to medium bedded argillaceous limestone and thick bedded to massive, grey orbitolina bearing limestone
543	Ktr	Grey oolitic and bioclastic orbitolina limestone
544	Ktzl	Thick bedded to massive, white to pinkish orbitolina bearing limestone
545	Ku	Upper cretaceous, undifferentiated rocks
546	Kuabv	Late-Cretaceous andesitic and basaltic lava flows
547	Kuavs	Andesitic Volcano sedimentary
548	Kuf	Unknown
549	Kuf	Flysch type sediments including shale, sandstone, limestone and conglomerate
550	Kufsh	Mudstone, shale and sandstone
551	Kuft	Flysch turbidites
552	Kufv	Flysch-volcanic rocks
553	Kugr	Granite and granodiorite
554	Kugr-di	Granite to Diorite
555	Kupl	Globotrunca limestone
556	Kur	Radiolarian chert and shale
557	Kurl	Undifferentiated pelagic limestone and radiolarian chert
558	Kus	Flysch turbidite sandstone with interbed calcareous mudstone and shale
559	Kussh	Dark grey shale
560	Kussh	Dark grey shale
561	l	Massive, recrystalized limestone with minor phyllite and schist
562	L.E-Oa. bv	Andesitic to basaltic volcanic
563	L.E-Oa. bvt	Andesitic to basaltic volcanic tuff
564	L.E-Oav	Andesitic volcanic
565	L.E-Obv	Basaltic volcanic
566	L.E-Od.at	Dacitic to andesitic tuff
567	L.E-Od. av	Dacitic to andesitic volcanic
568	L.E-Od. avb	Dacitic to andesitic volcano breccia
569	L.E-Od. avt	Dacitic to andesitic volcanic tuff
570	L.E-Odi	Diorite
571	L.E-Odsv	Late Eocene-Early Oligocene rhyolitic to rhyodacitic subvolcanic rocks
572	L.E-Odv	Rhyolitic to rhyodacitic volcanic
573	L.E-Of	Feldespatoidal intrusive rock
574	L.E-Ogr	Late Eocene-Early Oligocene granite
575	Lake	Unknown
576	lv	Listvinite
577	M1-2f	Thickly bedded sandstone with interbedded siltstone and shale
578	M1-2m	Shale, gypsiferous shale, gypsiferous mudstone and silty shale with minor sandstone and limestone

Soil order legend

ID	Soil order
1	Inceptisols/Vertisols
2	Inceptisols
3	Entisols/Inceptisols
4	Entisols/Aridisols
5	Aridisols
6	Rock outcrops/ Inceptisols
7	Rock outcrops/Entisols
8	Playa
9	Rocky lands
10	Kalut
11	Dune lands
12	Marsh
13	Coastal sands
14	Bad lands
15	Mollisols
16	Water body
17	Urban
18	Salt plug
19	Salt flats
20	Alfisols